# Bathymetric Controls on Calving Processes at Pine Island Glacier

Jan Erik Arndt[1], Robert D. Larter[2], Peter Friedl[3], Karsten Gohl[1], and Kathrin Höppner[3]

[1]Alfred Wegener Institute Helmholtz Centre for Polar and Marine Research, Am Handelshafen 12, 27570 Bremerhaven, Germany
5  [2]British Antarctic Survey, High Cross Madingley Road, Cambridge, CB3 0ET, UK
[3]German Aerospace Center (DLR), German Remote Sensing Data Center, Oberpfaffenhofen, Münchener Str. 20, 82234 Wessling, Germany

*Correspondence to*: Jan Erik Arndt (Jan.Erik.Arndt@awi.de)

**Abstract.** Pine Island Glacier is the largest current Antarctic contributor to sea level rise. Its ice loss has substantially increased
10  over the last 25 years through thinning, acceleration and grounding line retreat. However, the calving line positions of the stabilizing ice shelf did not show any trend within the observational record (last 70 years) until calving in 2015 led to unprecedented retreat and changed alignment of the calving front. Bathymetric surveying revealed a ridge below the former ice shelf and two shallower highs to the north. Satellite imagery shows that ice contact on the ridge likely was lost in 2006 but was followed by intermittent contact resulting in back stress fluctuations on the ice shelf. Continuing ice shelf flow also led to
15  occasional ice shelf contact with the northern bathymetric highs, which initiated rift formation that led to calving. The observations show that bathymetry is an important factor in initiating calving events.

## 1 Introduction

Ice loss from Pine Island Glacier (PIG) is currently the largest contribution to sea-level rise from any single Antarctic glacial outlet (Shepherd et al., 2012). Ice losses from PIG and neighbouring outlets in the eastern Amundsen Sea Embayment, which
20  collectively drain about a third of the West Antarctic Ice Sheet, now account for about 5-10% of current sea-level rise (Shepherd et al., 2012;Rignot et al., 2008;Lee et al., 2012). Remote sensing data show that ice loss in this sector has increased greatly over the past 25 years through ice thinning and flow acceleration that is triggered by thinning of the floating ice shelves at rates between 3.9 and 5.3 m yr-1 (Rignot, 2008;Rignot et al., 2008;Rignot et al., 2014;Pritchard et al., 2009;Wingham et al., 2009). Integration of remote sensing data with oceanographic observations shows that this thinning results from enhanced
25  basal melting driven by incursion of relatively warm Circumpolar Deep Water (CDW) onto the continental shelf (Jacobs et al., 1996;Jacobs et al., 2011;Pritchard et al., 2012;Nakayama et al., 2013;Dutrieux et al., 2014a). Precise dating of changes in sediment cores recovered beneath PIG ice shelf indicates that the present phase of thinning and retreat was initiated in the 1940s (Smith et al., 2017), which is consistent with a hypothesis that CDW incursion increased at this time driven by wind stress changes associated with a large El Niño event between 1939–42 (Steig et al., 2012). In the 1990s the grounding line of
30  PIG was located on a ridge in the bed which rises to 700–800 m below sea level along its crest (Rignot et al., 2014;Joughin et al., 2016). Between 1992 and 2011 the grounding line retreated 31 km at the centre of PIG, migrating to a position on the bed

400 m deeper than in 1992 (Rignot et al., 2014). Upstream of the 2011 grounding line position the bed steadily increases in depth for more than 200 km (Fretwell et al., 2013). Glaciological theory and ice sheet models imply that grounding lines are unstable on such upstream-deepening beds (Favier et al., 2014;Katz and Worster, 2010;Weertman, 1974;Schoof, 2007), raising the prospect of runaway retreat along the trunk of PIG. Ice shelves downstream of the grounding line have a buttressing effect

5    on the grounded portion of such marine based ice streams and, therefore, the ice shelf at the downstream end of PIG is an important factor in maintaining its stability (Schoof, 2007;Fürst et al., 2016;Gudmundsson, 2013).

Despite the thinning and flow acceleration of PIG, and sustained, rapid thinning of the ice shelf over at least the past 25 years the position of the ice front had not shown any clear trend over 68 years of observations prior to 2015 (Bindschadler, 2002;MacGregor et al., 2012;Rignot, 2002; Fig. 1). In 2011 a rift developed that two years later, in November 2013, resulted

10   in calving of the 720 sq. km iceberg B-31 (Bigg et al., 2014). This calving front remained in an orientation similar to that of calving fronts through previous decades, which were consistently aligned 10–30° east of north (Rignot, 2002;MacGregor et al., 2012). Less than two years later, in August 2015, another major calving event (580 sq. km area) resulted in retreat of the northern part of the ice front to a position a further ~15 km upstream of where it had been after the 2013 calving, representing the most retreated ice front position observed up until that time (Jeong et al., 2016). The August 2015 event also resulted in a

15   realignment of the calving front to 55° east of north, parallel to the trend of new rifts in the ice shelf, 'R1' and 'R2', that were first observed in 2013-14 (Jeong et al., 2016). This new retreated and realigned calving line location has been recently reconfirmed by a calving event in September 2017 (280 sq. km area) that resulted in a calving front location nearly identical to the one in 2015.

The recent retreat of the calving front presented an opportunity during research cruise PS104 on RV *Polarstern* in February

20   2017 to survey the bathymetry of a ~370 sq. km area that had previously been covered by ice shelf throughout the period for which observational records exist. This area included a bathymetric high on which the northern part of the PIG ice shelf was pinned in the past, as previously recognized (Bindschadler, 2002;Rignot, 2002). Here we present multibeam bathymetry data from this newly exposed area together with Synthetic Aperture Radar (SAR) and optical imagery to investigate the role of this pinning point and other bathymetric featrures in the calving development of the PIG ice shelf.

## 2 Methods

### 2.1 Swath Bathymetry

Swath bathymetric data of RV *Polarstern* research cruise PS104 have been acquired with the hull-mounted Teledyne Hydrosweep DS3 system. This system uses a transmitting frequency of 15.5 kHz and has 0.2 % of the water depth vertical measurement accuracy in the centre beam and up to 0.5 % of the water depth for the outer beams. The data have been processed,

30   sound-velocity corrected and edited for outliers with the CARIS HIPS and SIPS software. The sound velocity profile used was obtained from a conductivity-temperature-depth cast carried out nearby shortly before the survey. Data gridding was performed at 25 m resolution with a weighted moving average gridding algorithm in the software QPS Fledermaus.

## 2.2 Remote Sensing

Satellite data acquired with different Synthetic Aperture Radar (SAR) sensors on board of the European Remote Sensing Satellite 2 (ERS-2), RADARSAT-1, the Advanced Land Observing Satellite 1 (ALOS-1), Envisat, TerraSAR-X, TanDEM-X, and Sentinel-1A/B as well as data of the optical Advanced Spaceborne Thermal Emission and Reflection Radiometer (ASTER)

5    were used in order to derive a time series of images from 2002 to 2017 over the region near the bathymetric ridge (Table 1). For the SAR data, intensity images were extracted from data acquired in Single Look Complex (SLC) format. In order to obtain roughly square pixels on the ground and to reduce speckle noise, multi-looking was performed by applying sensor dependent multi-look factors in range and azimuth direction (Table 1).The resulting Multi-Look Intensity (MLI) images were radiometrically calibrated, geocoded and orthorectified. For orthorectification the Bedmap2 Digital Elevation Model (Fretwell

10    et al., 2013) resampled to a 100 m spatial resolution served as a source of topographic information.

## 2.3 Ice Thickness Data

We considered trying to estimate the time of ice shelf contact loss with the bathymetric high by comparing the bathymetry data to ice shelf thickness measurements. However, thickness estimates from radar surveys (Vaughan et al., 2012) and those calculated from the ice shelf freeboard measured by satellite altimetry (Chuter and Bamber, 2015;Griggs and Bamber, 2011)

15    show differences up to ~100 m. These differences probably result largely from uncertainties in the appropriate firn depth corrections and flexural effects that cause some areas of the ice shelf to deviate from hydrostatic equilibrium, but regardless of their cause they show that ice shelf thickness estimates are too uncertain to determine the timing of ice contact loss.

## 3 Results

### 3.1 Bathymetry

20    The high-resolution bathymetry of the previously ice-shelf covered area reveals an ENE to WSW trending ridge that extends 10 km from underneath the Northern Ice Shelf into Pine Island Bay (Fig. 2). While water depths in the bay are up to 1080 m in its centre, the shallowest point on the ridge is at a water depth of only 375 m. The deepest section of the crest of the ridge is at 440 m water depth. On its edges, the ridge drops abruptly within a few hundred meters down to more than 700-800 m water depth. Sets of streamlined seafloor landforms are visible in Pine Island Bay south of the ridge, north of the ridge and locally

25    on the ridge itself. The orientations of these streamlined landforms are different in each of the locations. South of the ridge, their orientation is from ESE to WNW throughout the surveyed area. North of the ridge, their orientation is ENE to SWS changing to ESE to WNW farther to the west. The streamlined features on the ridge itself are oriented SE to NW, resembling the direction of modern-day satellite observed ice-shelf movement (Jeong et al., 2016;Rignot et al., 2011). Two other bathymetric highs are located 15 km north and 20 km northwest of the bathymetric ridge (Fig. 2a). The western bathymetric

high A reaches depths shallower than 350 m. The eastern bathymetric high B has a lowest measured depth of less than 250 m and likely continues to the north where a grounded portion of the Northern Ice shelf is present.

## 3.2 Ice Shelf Contact to Bathymetric Ridge

Analysis of the satellite data shows that an ice rumple was present at the location of the shallowest part of the bathymetric ridge in the past (Fig. 3, see also Supplementary Movie S1). These rumples were previously observed in Landsat images between January 1973 and January 2001 by Bindschadler (2002) who also described rifts oriented perpendicular to ice-shelf flow forming immediately downstream of the rumple. Three of these ~3 km long rifts are still observed about 5 km downstream in an image collected in March 2002 (Fig. 3a), but since then no intense rifting is observed and only more subtle rifts are detected downstream of the rumple. However, in images collected over the following three years, the ice rumple continues to be observed above the bathymetric ridge and irregularities in the ice surface originating there are carried downstream, indicating continued ice-shelf contact. The ice rumple is observed for the last time in March 2005 (Fig. 3b). A rift oriented in NNW-SSE direction above the bathymetric ridge is visible in January 2006 (Fig. 3c). Similar rifting is not visible on satellite images of younger age. Therefore, this indicates that the ice shelf thinned sufficiently so that either ice contact became too light to produce imprints on the ice surface or that the ice shelf did not ground at all any more.

In the timespan since reduced ice contact is documented, ice rifting increasingly took place further to the east near Evans Knoll with rifts pre-dominantly being oriented in N-S direction. In the last years before the 2015 calving event, the rifted northern margin flowed across the bathymetric ridge with no indication of ice contact (Fig. 3d). To the north, an ice mélange developed between PIG ice shelf and the Northern Ice Shelf, along the downstream projection of PIG's lateral shear zone, and remained present until it disintegrated in 2014 and early 2015 immediately prior to the 2015 calving event (Jeong et al., 2016, see also Supplementary Movie S2).

## 3.3 Calving Events

Since the last evident ice contact between ice shelf and bathymetric ridge in 2006, four major calving events took place at PIG (Fig. 4 and 5). In 2007, the calving front was located approximately 8 km west of the pinning point and produced a curved calving line (Fig. 4a). At the time of rift initiation, the northern front of the PIG ice shelf moved above bathymetric high A. Four years later, in 2011, a similar rift with curved shape appeared further to the east, this time only 2 km west of the pinning point (Fig. 4b). At this time, very dense ice mélange consisting of thick fragments of the rifted PIG margin and of the Northern Ice Shelf was present northwest of the rift between bathymetric high B and PIG. The rift further opened from north to south and led to calving of iceberg B-31 in 2013. In 2015, the calving occurred along one of the pair of rifts ('R1') that had appeared in the ice shelf 1-2 years earlier (Jeong et al., 2016), and produced a calving front located east of the former pinning point that was linear and aligned 55° east of north (Fig. 4c). The calved iceberg rapidly broke apart at least within a month. Icebergs originating from the southern part of the ice shelf immediately drifted westward out of the region. The northern iceberg (~115 sq. km), however, remained above the bathymetric ridge for a year slowly rotating 90° in clockwise direction around a point

on the high during this time (Fig. 4c and Supplementary Movie S2). Two years later, in September 2017, calving occurred along rift 'R2' (Fig. 5). The new calving front varied by less than 1 km from the calving line position of the 2015 event. Immediately before the calving, the ice shelf front was still >4 km southeast of the bathymetric ridge. The calved iceberg broke apart into >15 parts (each ≤50 sq. km) within only 2 months. A new rift 'R3' located approximately 4 km upstream of the
5  calving line with similar orientation as 'R1' and 'R2' became visible the first time in a satellite image taken on the 13th of October 2017 (inset of Fig.5).

## 4 Discussion

The streamlined morphology visible in the new bathymetry data resembles drumlins and glacial lineations as discovered in other formerly glaciated areas. These features were produced by past ice movement with their orientation indicating the
10  direction of ice-flow at the time when they were produced (Graham et al., 2009). The drumlins and lineations located in the deeper parts adjacent to the ridge show a converging flow of ice west of the ridge (Fig. 2a). In the southern part of the newly-surveyed area ice originated from PIG. In the northern part ice originated from a tributary located north of Evans Knoll. Dated sediment cores located ~100 km downstream of the modern grounding line in inner Pine Island Bay suggests that the grounding line retreated from this position before at least 11.7 cal kyrs B.P. (Hillenbrand et al., 2013). Rapid thinning of PIG at around 8
15  cal kyrs B.P has been documented by investigation of cosmogenic exposure ages of rocks from the hinterland (Johnson et al., 2014). Hence, a grounded ice stream setting forming drumlins and lineations in the deep sections of the trough was likely last active before about 8 ka. The lineations on the bathymetric ridge, however, likely were formed at a later stage when the ice sheet had further thinned and retreated as indicated by their slightly different orientation. This angle coincides with the modern-day ice flow direction of PIG ice shelf and implies that the lineations were formed by the ice shelf while it remained grounded
20  on the ridge until the ice shelf sufficiently thinned or retreated. Nevertheless, we cannot rule out that multiple glacial cycles were needed to form these lineaments as the ridge crest probably consists of resistant bedrock. Therefore, the lineaments alternatively may represent the average ice flow direction during these glacial cycles.

Pinning point loss probably resulted from rapid thinning of the ice shelf that has occurred over the past two decades, exceeding 5 m yr$^{-1}$ in recent years (Pritchard et al., 2012;Rignot et al., 2013). The time series of satellite imagery suggests that the ice
25  shelf lost contact with the shallowest part of the bathymetric ridge at some time in 2006, or at least contact was too weak since then to produce a surface expression (Fig. 3). At least weak or intermittent ice contact was also still present until the 2015 calving event when a calved iceberg remained stationary on top of the ridge for about a year (Fig. 4c and Supplementary Movie S2). These circumstances provide a relatively good timing constraint for the loss of ice shelf contact. Hence, the glacial lineations located on top of the bathymetric ridge were formed, or at least ice covered, until the last decade, making them some
30  of the youngest submarine glacial landforms mapped in Antarctica. In addition, this detailed chronological information makes the bathymetric ridge a possible target to study benthic biological recolonization (Gutt et al., 2011) in the Pacific realm of West Antarctica.

Since 2006 four major calving events took place at PIG in 2007, 2013, 2015 (Fig. 4), and 2017 (Fig. 5). These events were different in comparison to calving events before. The 2007 and 2013 calving events for the first time occurred along curved calving lines, which had not been observed before (Fig. 1). The 2015 event resulted in the most retreated calving position observed and reorientation of the calving front to 55° east of north, which is 25° to 45° clockwise in comparison to previous

5 calving fronts (Fig. 1). This reorientation of the calving front was reconfirmed by the 2017 event. Pinning point loss results in reduced back stress to the ice shelf through reduction of basal drag (Favier et al., 2014) and the topography of an ice-shelf cavity is important for internal water exchange (De Rydt et al., 2014). Therefore, in the following we evaluate how the bathymetric ridge and the two highs A and B affected the development of the PIG ice shelf.

Less than a year after imprints of ice contact with the bathymetric ridge had been imaged in satellite data for the last time (Fig.

10 3), a calving event led to an exceptional calving front geometry in 2007 (Fig. 1 and 4a). The satellite images do not reveal a direct link between ice contact loss at the bathymetric ridge and this calving event. However, the coincidence in the timing of arrival of the northernmost part of the PIG ice shelf front at bathymetric high A and the propagation of the calving rift SSE from the high is evident (Supplementary Movie S1). The contact of the ice shelf front with bathymetric high A in the northwest imparted back stress to the northernmost part of the ice shelf and, hence, rift propagation occurred between ice to the SE of

15 the high that was subject to this back stress and ice to its south that was not restrained (Fig. 4a).

In the following years, ice shelf rifting increasingly took place further to the east (Fig. 3) where it ceases to be constrained by topography around Evans Knoll (Fig. 1), indicating that stresses were increasingly being released here rather than at the bathymetric ridge. The northern part of the large rift that formed in 2011 coincides with the N-S direction of the rifts forming near Evans Knoll (Fig. 3b and 4b). The rift propagated southwards and formed the 2013 calving front indicating that the stress

20 release played a role for this calving event. In addition, before rift formation the very dense mélange of icebergs north of the bathymetric ridge became trapped between the PIG and the Northern Ice Shelf that partly rested on bathymetric high B. In a similar way to direct ice shelf contact with a bathymetric high observed in 2007, this configuration imposed back stress on the northern section of the PIG ice shelf and influenced the position of the 2011 rift. Hence, the bathymetric highs A and B played an important role in both calving events that resulted in a curved calving front by inducing sudden back stress to the PIG ice

25 shelf, either directly via ice shelf contact to the ridge in 2007, or indirectly via trapping a dense ice mélange in 2011.

Before the 2015 calving event, change of ice-flow velocity and direction from 2013-2014 to 2014-2015 (Jeong et al., 2016) shows that the northern section that later on became the stationary iceberg behaved differently compared to the calved central and southern part. In the northern section, (1) ice flow velocity stayed nearly the same instead of increasing and (2) ice flow direction rotated 2–3° clockwise instead of more or less remaining the same. This observation could indicate slight contact of

30 ice with the bathymetric ridge in Fig. 2b, which was located on the northernmost edge of the ice shelf by then. This is supported by the observation of the stationary northern iceberg (Fig. 4c) that can only be explained by bottom contact. Ice contact even before the calving event, therefore, would explain the observed reduced flow speed in the northern ice shelf section and the general westward flow direction of the ice shelf would have resulted in clockwise rotation with an anchor point in the north. Radar and upward-looking sonar data showed that the base of PIG ice shelf is highly irregular (Vaughan et al., 2012;Dutrieux

et al., 2014b) and, therefore, suggest that the initial loss of ice contact likely would be followed by a phase of intermittent contact. Hence, the irregular ice shelf thickness likely led to re-grounding on the bathymetric ridge and triggered the different ice flow behaviour in the northern part. Furthermore, this asymmetry probably explains the rapid break-up of the calved ice due to the different rotation and forcing in the northern section.

5    The resulting re-oriented calving line of the 2015 event, however, was pre-dominantly controlled by rift 'R1' and by the disintegration of ice mélange between PIG and the Northern Ice Shelf as described by Jeong et al. (2016). This is supported by the 2017 calving event that was controlled by rift 'R2' (Fig. 1) with the calved part being more than 4 km away from the former pinning point (Supplementary Fig. S3). The R1 and R2 rifts were hypothesized by Jeong et al. (2016) to originate from basal crevasses filled by warm ocean waters. Nevertheless, the pinning point loss could have contributed to the formation of

10   these rifts through back stress changes following the initial pinning point loss around 2006 and during the period of intermittent ice contact that we have showed continued until the 2015 calving event. The alignment of these rifts between the new outermost pinning point in the north, near Evans Knoll, and the position where a tributary glacier flows into the ice shelf in the south, is consistent with this hypothesis. This observation will be an important consideration for improved understanding and modelling of the rift formation process.

15   Due to its morphology, in addition, the bathymetric ridge possibly played a role in clearing the ice mélange. Apart of an open marine gateway for ice into Pine Island Bay, a force is needed to push the ice mélange into the bay. Iceberg trajectories are predominantly steered by currents and wind (Death et al., 2006). Therefore, a water exchange from the ice shelf cavity across the bathymetric ridge would support flushing the trapped icebergs westward. The ridge, being continuously shallower than 450 m, in combination with the ice shelf and icebergs trapped in the mélange (reaching drafts of hundreds of meters), however,

20   would have limited this kind of water exchange. After sufficient thinning took place, the water column possibly reached a threshold that enabled sufficient circulation of water to allow ice mélange disintegration.

The current calving front aligns between the new downstream-most pinning point in the north, near Evans Knoll, and where the ice shelf is under pressure from a tributary ice stream flowing into it in the south. In the decades before, when other pinning points including the discovered bathymetric ridge were active in the north, this was also the case (Fig. 1). This correlation

25   suggests that the final pinning/constriction points are an important control on the orientation of the calving line of PIG. However, in a thinner ice shelf, crevasses that developed in the glacier upstream of the grounding line will penetrate a greater fraction of the total thickness, and therefore they are more likely to control calving positions (Yu et al., 2017;Bassis and Jacobs, 2013;Bassis and Walker, 2011). Hence, we cannot exclude that the change in calving line orientation is a result of thinning and ocean melting of basal crevasses as suggested by Jeong et al. (2016), possibly enhanced by backstress variations due to

30   intermittent ice contact to the bathymetric ridge between 2006 and 2015, and is not solely constrained by outermost pinning points.

Konrad et al. (2017) show how changes to the ice shelf and grounding line region of PIG and other Amundsen Sea Embayment glaciers propagate upstream on a timescale of a few years. Thus, the recent reduction of back stress can be expected to propagate to the grounded trunk of PIG, causing further acceleration of flow, and thus further dynamic thinning. Accordingly,

a re-stabilization of the ice shelf due to re-pinning at a ridge e.g. by a very rapid advance or thickening of the ice shelf cannot be expected in the foreseeable future, at least for as long as rapid basal melting driven by continued CDW incursion continues. Instead, the ice shelf calving line seems to have made an irreversible step to a new position and orientation in 2015, which has been confirmed in 2017, following progressive detachment from the pinning point over the previous decade. We do not expect

5    further significant rapid calving line retreat in the next few years. The northern margin is now stabilized by a pinning point near Evans Knoll, which rises above sea level and where the nearby ice-shelf thickness is about 450 m, and the southern margin is stabilized by thick tributary ice inflow (Fretwell et al., 2013). Nevertheless, continued rapid ice shelf thinning as observed in other studies (Pritchard et al., 2012;Rignot et al., 2013) and as confirmed by our observation of pinning point loss (Fig. 3) will further destabilise the PIG ice shelf in the future and at some stage is expected to lead to calving occurring even further

10   upstream. Rapid iceberg disintegration after the two most recent calving events within 1-2 months into smaller sized icebergs (maximum size ~115 sq. km in 2015 and ~50 sq. km in 2017, Fig. 4 and 5) in comparison to previous calving events that resulted in stable large icebergs, e.g. B-31 (720 sq. km, Bigg et al., 2014), possibly reflect this destabilizing trend. The newly discovered rift R3 (inset of Fig. 5) likely will trigger the next calving event. In comparison to the 2015 (10-20 km) and 2017 (8 km) calving event R3 is located only 4 km upstream of the current calving front therefore indicating that the trend to smaller

15   sized icebergs will persist.

## 5 Conclusions

- Multibeam bathymetry data from a previously ice shelf covered area revealed a bathymetric ridge that rises to 375 mat its shallowest point and two shallower bathymetric highs A and B to the north.

- The bathymetric ridge acted as a pinning point to the PIG until 2006. Between 2006 and 2015 ice contact likely
20      persisted at least intermittently and induced variable back stress to PIG.

- Four calving events occurred since 2006. The 2007 event is a result of back stress induced by bathymetric high A to the north-eastern part of PIG after ice front advance to the high. The 2013 event resulted from back stress induced by a dense ice mélange trapped between PIG and bathymetric high B. The 2015 event was triggered by clearing of a northern ice mélange and rift R1 as suggested by Jeong et al. (2016), the 2017 event was triggered by rift R2 and the
25      next calving likely will occur along the newly identified rift R3. These rifts align between the terminal ice-shelf stabilising points to the north and south and calving occurred when they migrated past the stabilising points. We suggest that (a) reduced and variable back stress after 2006 favoured the formation of these rifts, (b) the clearing of the ice mélange was constrained by water flux over the bathymetric ridge and (c) that light ice shelf contact to the ridge initiated the final breakup in 2015.

30   - In the last decade, the size of calved icebergs has shrank and their speed of disintegration accelerated possibly due to ice-shelf destabilization by continuous rapid ice-shelf thinning.

*Data availability.* The bathymetric data are available at https://doi.org/10.1594/PANGAEA.881546. The processed satellite images are available upon request from the authors.

*Author contributions.* J.E.A., R.D.L. and K.G. developed the concept of this paper. J.E.A. was responsible for bathymetry data acquisition and processing. P.F. and K.H. were responsible for satellite data acquisition and processing. J.E.A. and R.D.L. led the writing of this paper and all authors contributed to the development of the paper.

*Competing interests.* The authors declare no competing interests

*Acknowledgements.* The TerraSAR-X acquisitions during RV *Polarstern's* expedition PS104 were provided by DLR through the TerraSAR-X science project OCE3373 (Fig. 1) and the TanDEM-X Science Proposal XTI_GLAC7015 (Fig. 4c, Movie S2 in supporting information). The ERS and Envisat data were provided free of charge by ESA via the Earth Observation Link (EOLi) client. Sentinel-1 data were downloaded from ESA`s Copernicus Open Access Hub. We thank JAXA for providing the ALOS PALSAR data and Matthias Braun (University of Erlangen-Nuremberg) for kindly sharing processed RADARSAT-1 intensity images. ASTER data from the L1B Orthorectifed Registered Radiance at the Sensor V003 Product (AST14OTH) was retrieved via the NASA Reverb portal. We thank the crew of RV *Polarstern* and the scientific staff on board during expedition PS104 for their help and assistance. We thank John B. Anderson and Seongsu Jeong for comments on a previous version of this manuscript and Seongsu Jeong for sharing the Sentinel S2A image showing rift R3. J.E.A. was funded by the Deutsche Forschungsgemeinschaft (DFG, German Research Foundation) – AR 1087/1-1. This study is part of the PACES II (Polar Regions and Coasts in the changing Earth System) programme of the Alfred-Wegener-Institut and the Polar Science for Planet Earth Programme of the British Antarctic Survey.

## References

Bassis, J. N., and Walker, C. C.: Upper and lower limits on the stability of calving glaciers from the yield strength envelope of ice, Proceedings of the Royal Society A: Mathematical, Physical and Engineering Science, 10.1098/rspa.2011.0422, 2011.

Bassis, J. N., and Jacobs, S.: Diverse calving patterns linked to glacier geometry, Nature Geosci, 6, 833-836, 10.1038/ngeo1887, 2013.

Bigg, G. R., Marsh, R. A., Wilton, D. J., and Ivchenko, V.: B31—a giant iceberg in the Southern Ocean, Ocean Challenge, 20, 32-34, 2014.

Bindschadler, R. A.: History of lower Pine Island Glacier, West Antarctica, from Landsat imagery, Journal of Glaciology, 48, 536-544, 10.3189/172756502781831052, 2002.

Chuter, S. J., and Bamber, J. L.: Antarctic ice shelf thickness from CryoSat-2 radar altimetry, Geophysical Research Letters, 42, 10,721-710,729, 10.1002/2015GL066515, 2015.

De Rydt, J., Holland, P. R., Dutrieux, P., and Jenkins, A.: Geometric and oceanographic controls on melting beneath Pine Island Glacier, Journal of Geophysical Research: Oceans, 119, 2420-2438, 10.1002/2013JC009513, 2014.

Death, R., Siegert, M. J., Bigg, G. R., and Wadley, M. R.: Modelling iceberg trajectories, sedimentation rates and meltwater input to the ocean from the Eurasian Ice Sheet at the Last Glacial Maximum, Palaeogeography, Palaeoclimatology, Palaeoecology, 236, 135-150, 10.1016/j.palaeo.2005.11.040, 2006.

Dutrieux, P., De Rydt, J., Jenkins, A., Holland, P. R., Ha, H. K., Lee, S. H., Steig, E. J., Ding, Q., Abrahamsen, E. P., and Schröder, M.: Strong Sensitivity of Pine Island Ice-Shelf Melting to Climatic Variability, Science, 343, 174-178, 10.1126/science.1244341, 2014a.

Dutrieux, P., Stewart, C., Jenkins, A., Nicholls, K. W., Corr, H. F. J., Rignot, E., and Steffen, K.: Basal terraces on melting ice shelves, Geophysical Research Letters, 41, 5506-5513, 10.1002/2014GL060618, 2014b.

Favier, L., Durand, G., Cornford, S. L., Gudmundsson, G. H., Gagliardini, O., Gillet-Chaulet, F., Zwinger, T., Payne, A. J., and Le Brocq, A. M.: Retreat of Pine Island Glacier controlled by marine ice-sheet instability, Nature Climate Change, 4, 117-121, 10.1038/nclimate2094, 2014.

Fretwell, P., Pritchard, H. D., Vaughan, D. G., Bamber, J. L., Barrand, N. E., Bell, R., Bianchi, C., Bingham, R. G., Blankenship, D. D., Casassa, G., Catania, G., Callens, D., Conway, H., Cook, A. J., Corr, H. F. J., Damaske, D., Damm, V., Ferraccioli, F., Forsberg, R., Fujita, S., Furukawa, T., Gogineni, P., Griggs, J. A., Hamilton, G., Hindmarsh, R. C. A., Holmlund, P., Holt, J. W., Jacobel, R. W., Jenkins, A., Jokat, W., Jordan, T., King, E. C., Krabill, W., Riger-Kusk, M., Tinto, K., Langley, K. A., Leitchenkov, G., Luyendyk, B. P., Matsuoka, K., Nixdorf, U., Nogi, Y., Nost, O. A., Popov, S. V., Rignot, E., Rippin, D., Riviera, A., Ross, N., Siegert, M. J., Shibuya, K., Smith, A. M., Steinhage, D., Studinger, M., Sun, B., Thomas, R. H., Tabacco, I., Welch, B., Young, D. A., Xiangbin, C., and Zirizzotti, A.: Bedmap2: Improved ice bed, surface and thickness datasets for Antarctica, The Cryosphere, 7, 375-393, 10.5194/tc-7-375-2013, 2013.

Fürst, J. J., Durant, G., Gillet-Chaulet, F., Tavard, L., Rankl, M., Braun, M., and Gagliardini, O.: The safety band of Antarctic ice shelves, Nature Climate Change, 6, 479-482, 10.1038/nclimate2912, 2016.

Graham, A. G. C., Larter, R. D., Gohl, K., Hillenbrand, C.-D., Smith, J. A., and Kuhn, G.: Bedform signature of a West Antarctic palaeo-ice stream reveals a multi-temporal record of flow and substrate control, Quaternary Science Reviews, 28, 2774-2793, 10.1016/j.quascirev.2009.07.003, 2009.

Griggs, J. A., and Bamber, J. L.: Antarctic ice-shelf thickness from satellite radar altimetry, Journal of Glaciology, 57, 485-493, 10.3189/002214311796905659, 2011.

Gudmundsson, G. H.: Ice-shelf buttressing and the stability of marine ice sheets, The Cryosphere, 7, 647-655, 10.5194/tc-7-647-2013, 2013.

Gutt, J., Barratt, I., Domack, E. W., d'Udekem d'Acoz, C., Dimmler, W., Grémare, A., Heilmayer, O., Isla, E., Janussen, D., Jorgensen, E., Kock, K.-H., Lehnert, L. S., López-Gonzáles, P., Langner, S., Linse, K., Manjón-Cabeza, M. E., Meißner, M., Montiel, A., Raes, M., Robert, H., Rose, A., Schepisi, E. S., Saucède, T., Scheidat, M., Schenke, H.-W., Seiler, J., and

Smith, C. R.: Biodiversity change after climate-induced ice-shelf collapse in the Antarctic, Deep Sea Research Part II: Topical Studies in Oceanography, 58, 74-83, 10.1016/j.dsr2.2010.05.024, 2011.

Hillenbrand, C.-D., Kuhn, G., Smith, J. A., Gohl, K., Graham, A. G. C., Larter, R. D., Klages, J. P., Downey, R., Moreton, S. G., Forwick, M., and Vaughan, D. G.: Grounding-line retreat of the West Antarctic Ice Sheet from inner Pine Island Bay, Geology, 41, 35-38, 10.1130/G33469.1, 2013.

Jacobs, S. S., Hellmer, H. H., and Jenkins, A.: Antarctic Ice Sheet melting in the southeast Pacific, Geophysical Research Letters, 23, 957-960, 10.1029/96GL00723, 1996.

Jacobs, S. S., Jenkins, A., Giulivi, C. F., and Dutrieux, P.: Stronger ocean circulation and increased melting under Pine Island Glacier ice shelf, Nature Geoscience, 4, 519-523, 10.1038/ngeo1188, 2011.

Jeong, S., Howat, I. M., and Bassis, J. N.: Accelerated ice shelf rifting and retreat at Pine Island Glacier, West Antarctica, Geophysical Research Letters, 43, 11,720-711,725, 10.1002/2016GL071360, 2016.

Johnson, J. S., Bentley, M. J., Smith, J. A., Finkel, R. C., Rood, D. H., Gohl, K., Balco, G., Larter, R. D., and Schaefer, J. M.: Rapid Thinning of Pine Island Glacier in the Early Holocene, Science, 343, 999-1001, 10.1126/science.1247385, 2014.

Joughin, I., Shean, D. E., Smith, B. E., and Dutrieux, P.: Grounding line variability and subglacial lake drainage on Pine Island Glacier, Antarctica, Geophysical Research Letters, 43, 9093-9102, 10.1002/2016GL070259, 2016.

Katz, R. F., and Worster, M. G.: Stability of ice-sheet grounding lines, Proceedings of the Royal Society A: Mathematical, Physical and Engineering Science, 466, 1597-1620, 10.1098/rspa.2009.0434, 2010.

Konrad, H., Gilbert, L., Cornford, S. L., Payne, A., Hogg, A., Muir, A., and Shepherd, A.: Uneven onset and pace of ice-dynamical imbalance in the Amundsen Sea Embayment, West Antarctica, Geophysical Research Letters, 44, 910-918, 10.1002/2016GL070733, 2017.

Lee, H., Shum, C. K., Howat, I. M., Monaghan, A., Ahn, Y., Duan, J., Guo, J.-Y., Kuo, C.-Y., and Wang, L.: Continuously accelerating ice loss over Amundsen Sea catchment, West Antarctica, revealed by integrating altimetry and GRACE data, EPSL, 321–322, 74-80, 10.1016/j.epsl.2011.12.040, 2012.

MacGregor, J. A., Catania, G. A., Markowski, M. S., and Andrews, A. G.: Widespread rifting and retreat of ice-shelf margins in the eastern Amundsen Sea Embayment between 1972 and 2011, Journal of Glaciology, 58, 458-466, 10.3189/2012JoG11J262, 2012.

Nakayama, Y., Schröder, M., and Hellmer, H. H.: From circumpolar deep water to the glacial meltwater plume on the eastern Amundsen Shelf, Deep Sea Research Part I: Oceanographic Research Papers, 77, 50-62, 10.1016/j.dsr.2013.04.001, 2013.

Pritchard, H. D., Arthern, R. J., Vaughan, D. G., and Edwards, L. A.: Extensive dynamic thinning on the margins of the Greenland and Antarctic ice sheets, Nature, 461, 971-975, 10.1038/nature08471, 2009.

Pritchard, H. D., Ligtenberg, S. R. M., Fricker, H. A., Vaughan, D. G., van den Broeke, M. R., and Padman, L.: Antarctic ice-sheet loss driven by basal melting of ice shelves, Nature, 484, 502-505, 10.1038/nature10968, 2012.

Rignot, E.: Ice-shelf changes in Pine Island Bay, Antarctica, 1947-2000, Journal of Glaciology, 48, 247-256, 10.3189/172756502781831386, 2002.

Rignot, E.: Changes in West Antarctic ice stream dynamics observed with ALOS PALSAR data, Geophysical Research Letters, 35, L12505, 10.1029/2008gl033365, 2008.

Rignot, E., Bamber, J. L., van den Broeke, M. R., Davis, C., Li, Y., van de Berg, W. J., and van Meijgaard, E.: Recent Antarctic ice mass loss from radar interferometry and regional climate modelling, Nature Geoscience, 1, 106-110, 10.1038/ngeo102, 2008.

Rignot, E., Mouginot, J., and Scheuchl, B.: Ice Flow of the Antarctic Ice Sheet, Science, 333, 1427-1430, 10.1126/science.1208336, 2011.

Rignot, E., Jacobs, S., Mouginot, J., and Scheuchl, B.: Ice-Shelf Melting Around Antarctica, Science, 341, 266-270, 10.1126/science.1235798, 2013.

Rignot, E., Mouginot, J., Morlighem, M., Seroussi, H., and Scheuchl, B.: Widespread, rapid grounding line retreat of Pine Island, Thwaites, Smith, and Kohler glaciers, West Antarctica, from 1992 to 2011, Geophysical Research Letters, 41, 3502-3509, 10.1002/2014GL060140, 2014.

Schoof, C.: Ice sheet grounding line dynamics: Steady states, stability, and hysteresis, J. Geophys. Res., 112, FS03S28, 10.1029/2006JF000664, 2007.

Shepherd, A., Ivins, E. R., A, G., Barletta, V. R., Bentley, M. J., Bettadpur, S., Briggs, K. H., Bromwich, D. H., Forsberg, R., Galin, N., Horwath, M., Jacobs, S., Joughin, I., King, M. A., Lenaerts, J. T. M., Li, J., Ligtenberg, S. R. M., Luckman, A., Luthcke, S. B., McMillan, M., Meister, R., Milne, G., Mouginot, J., Muir, A., Nicolas, J. P., Paden, J., Payne, A. J., Pritchard, H., Rignot, E., Rott, H., Sørensen, L. S., Scambos, T. A., Scheuchl, B., Schrama, E. J. O., Smith, B., Sundal, A. V., van Angelen, J. H., van de Berg, W. J., van den Broeke, M. R., Vaughan, D. G., Velicogna, I., Wahr, J., Whitehouse, P. L., Wingham, D. J., Yi, D., Young, D., and Zwally, H. J.: A Reconciled Estimate of Ice-Sheet Mass Balance, Science, 338, 1183-1189, 10.1126/science.1228102, 2012.

Smith, J. A., Andersen, T. J., Shortt, M., Gaffney, A. M., Truffer, M., Stanton, T. P., Bindschadler, R., Dutrieux, P., Jenkins, A., Hillenbrand, C. D., Ehrmann, W., Corr, H. F. J., Farley, N., Crowhurst, S., and Vaughan, D. G.: Sub-ice-shelf sediments record history of twentieth-century retreat of Pine Island Glacier, Nature, 541, 77-80, 10.1038/nature20136, 2017.

Steig, E. J., Ding, Q., Battisti, D. S., and Jenkins, A.: Tropical forcing of Circumpolar Deep Water Inflow and outlet glacier thinning in the Amundsen Sea Embayment, West Antarctica, Annals of Glaciology, 53, 19-28, 10.3189/2012AoG60A110, 2012.

Vaughan, D. G., Corr, H. F. J., Bindschadler, R. A., Dutrieux, P., Gudmundsson, G. H., Jenkins, A., Newman, T., Vornberger, P., and Wingham, D. J.: Subglacial melt channels and fracture in the floating part of Pine Island Glacier, Antarctica, Journal of Geophysical Research: Earth Surface, 117, n/a-n/a, 10.1029/2012JF002360, 2012.

Weertman, J.: Stability of the Junction of an Ice Sheet and an Ice Shelf, Journal of Glaciology, 13, 3-11, 10.3198/1974JoG13-67-3-11, 1974.

Wingham, D. J., Wallis, D. W., and Shepherd, A.: Spatial and temporal evolution of Pine Island Glacier thinning, 1995–2006, Geophysical Research Letters, 36, n/a-n/a, 10.1029/2009GL039126, 2009.

Yu, H., Rignot, E., Morlighem, M., and Seroussi, H.: Iceberg calving of Thwaites Glacier, West Antarctica: full-Stokes modeling combined with linear elastic fracture mechanics, The Cryosphere, 11, 1283-1296, 10.5194/tc-11-1283-2017, 2017.
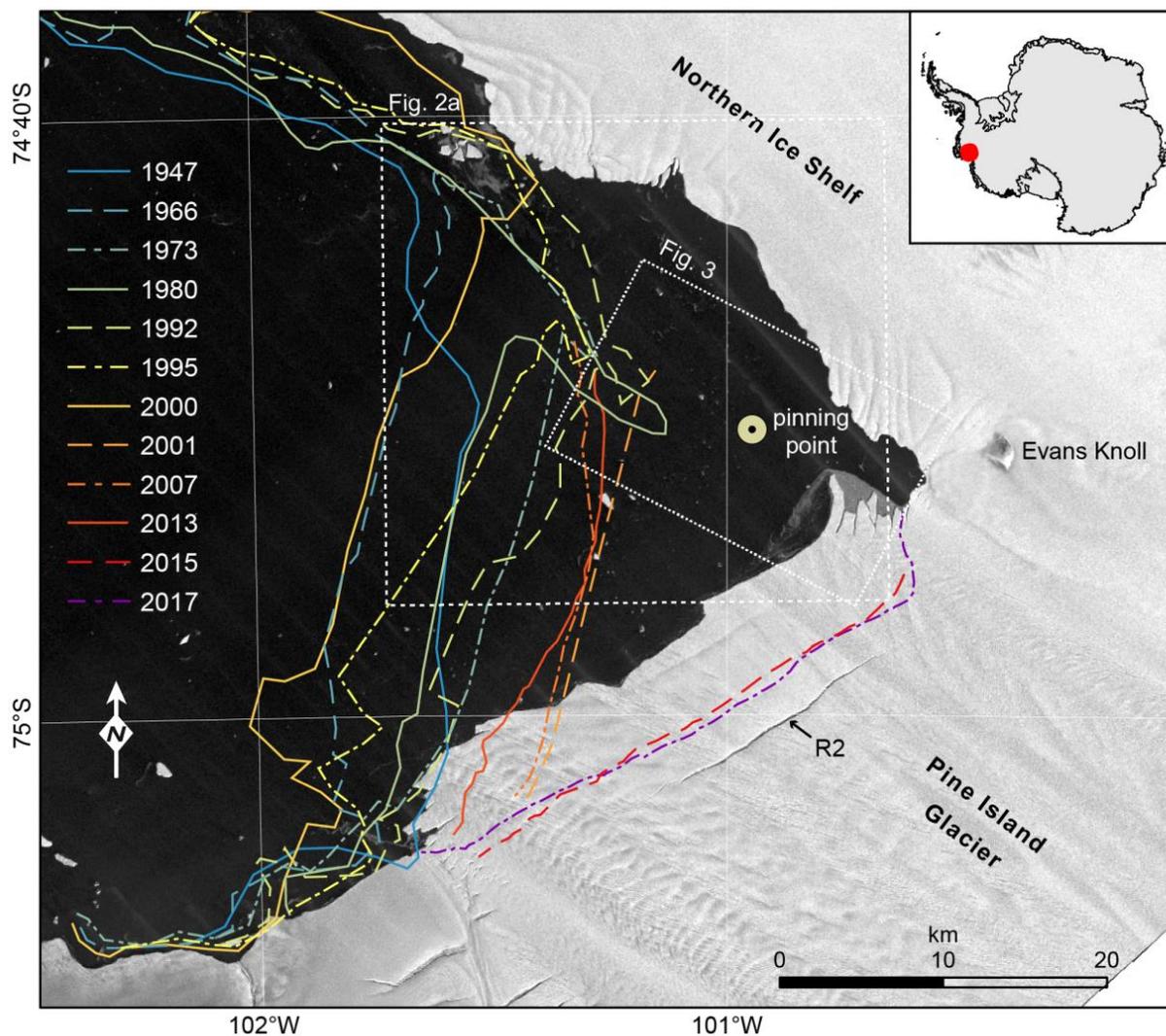
**Figure 1: Study area at the time of bathymetric data acquisition and past calving front positions. Satellite image (TanDEM-X ScanSAR L1b product (© DLR2017)) of Pine Island Bay from 17th Feb 2017 at 09:36 UTC and calving front positions over the last 70 years (1947-2001 taken from Rignot (2002), later positions are from this study), note the reoriented calving front in 2015. The dot denotes the location of the former pinning point were a bathymetry survey during RV *Polarstern* expedition PS104 revealed a ridge (see Figure 2). R2 is a rift previously described by Jeong et al. (2016). Inset map marks the location in Antarctica.**
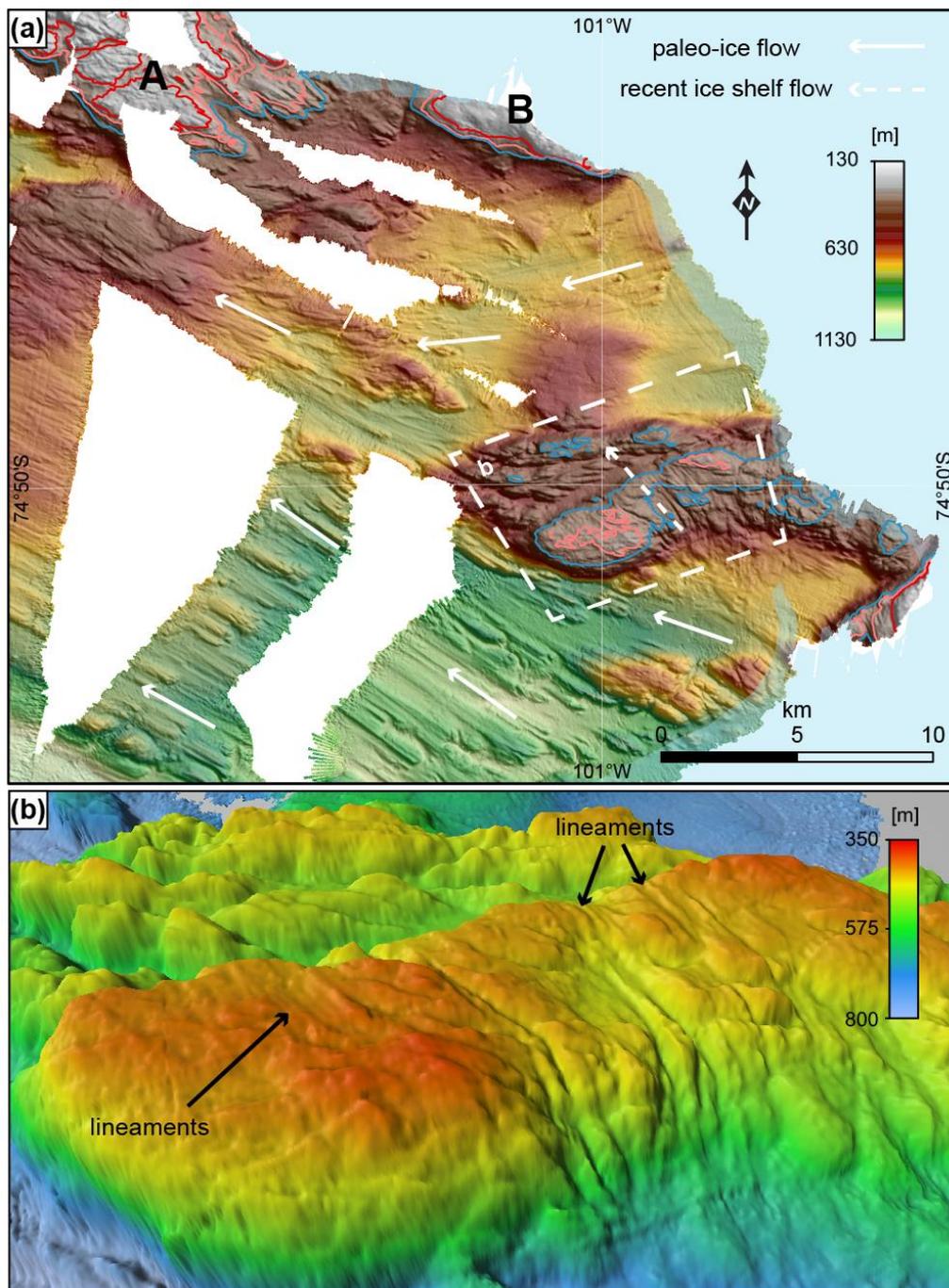
**Figure 2: Bathymetry of submarine ridge and adjacent seafloor at 25 m grid resolution. (a) Hill-shaded plan view with 350 m (dark red), 400 m (light red) and 450 m (blue) contours. Note the shoal areas in the northwest, labelled A and B. Paleo-ice flow inferred from drumlins and lineations shown by white arrows and direction of recent ice-shelf flow shown by dashed arrows. Semi-transparent blue area delineates ice covered area at time of data acquisition as shown in Figure 1. (b) 3D view of submarine ridge showing subtle lineaments oriented in the same direction as recent ice-shelf flow on its crest.**
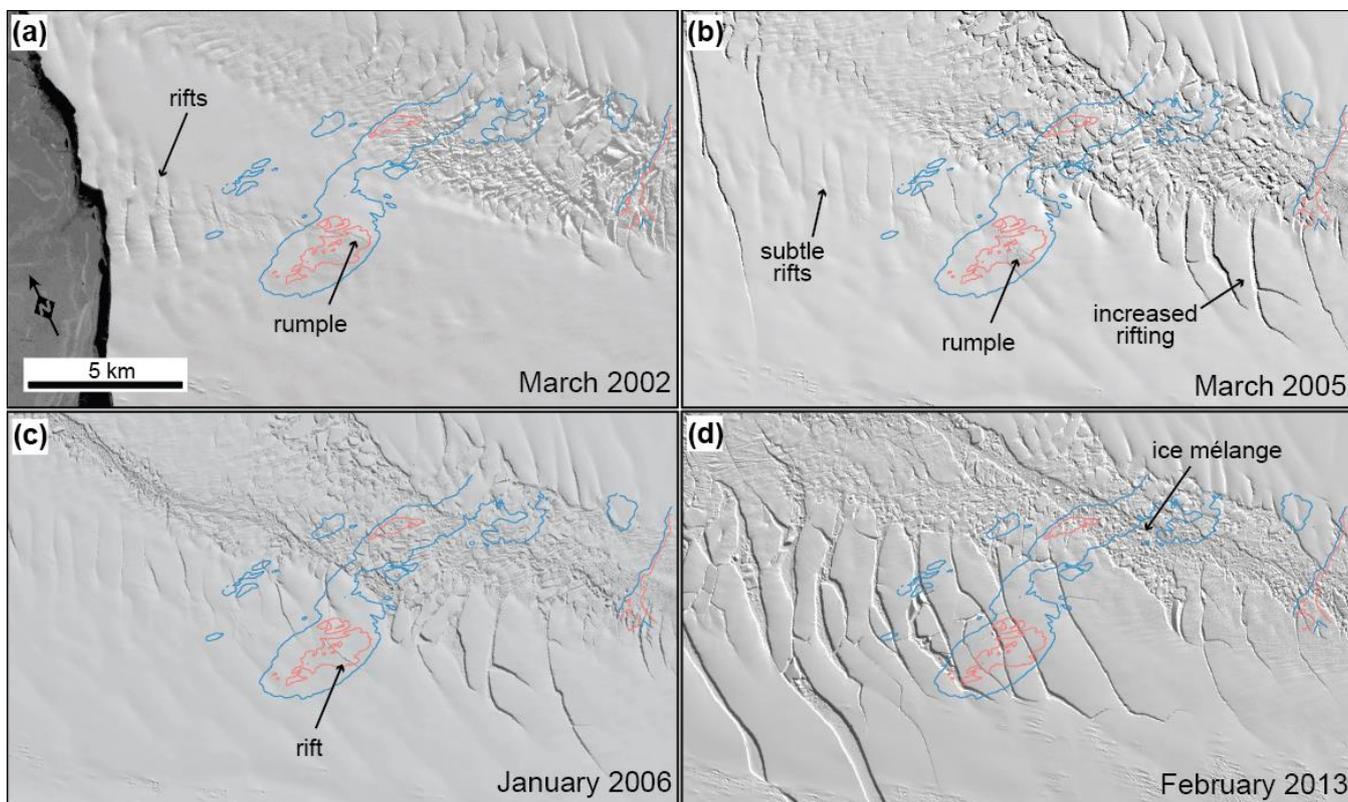
**Figure 3: Time series of ASTER satellite images taken from the area of the submarine ridge. Lines indicate depth contours of 400 m (red) and 450 m (blue). (a) Taken on 28th of March 2002, note the ice rumple on top of the ridge. (b) Taken on 1st of March 2005, note continued ice rumple and increased rifting in the east. (c) Taken on 18th of January 2006, note the rift forming on top of the ridge. (d) Taken on 10th of February 2013, note the absence of ice irregularities on top of the ridge, continuous intense rifting to its east, and ice mélange to its north.**
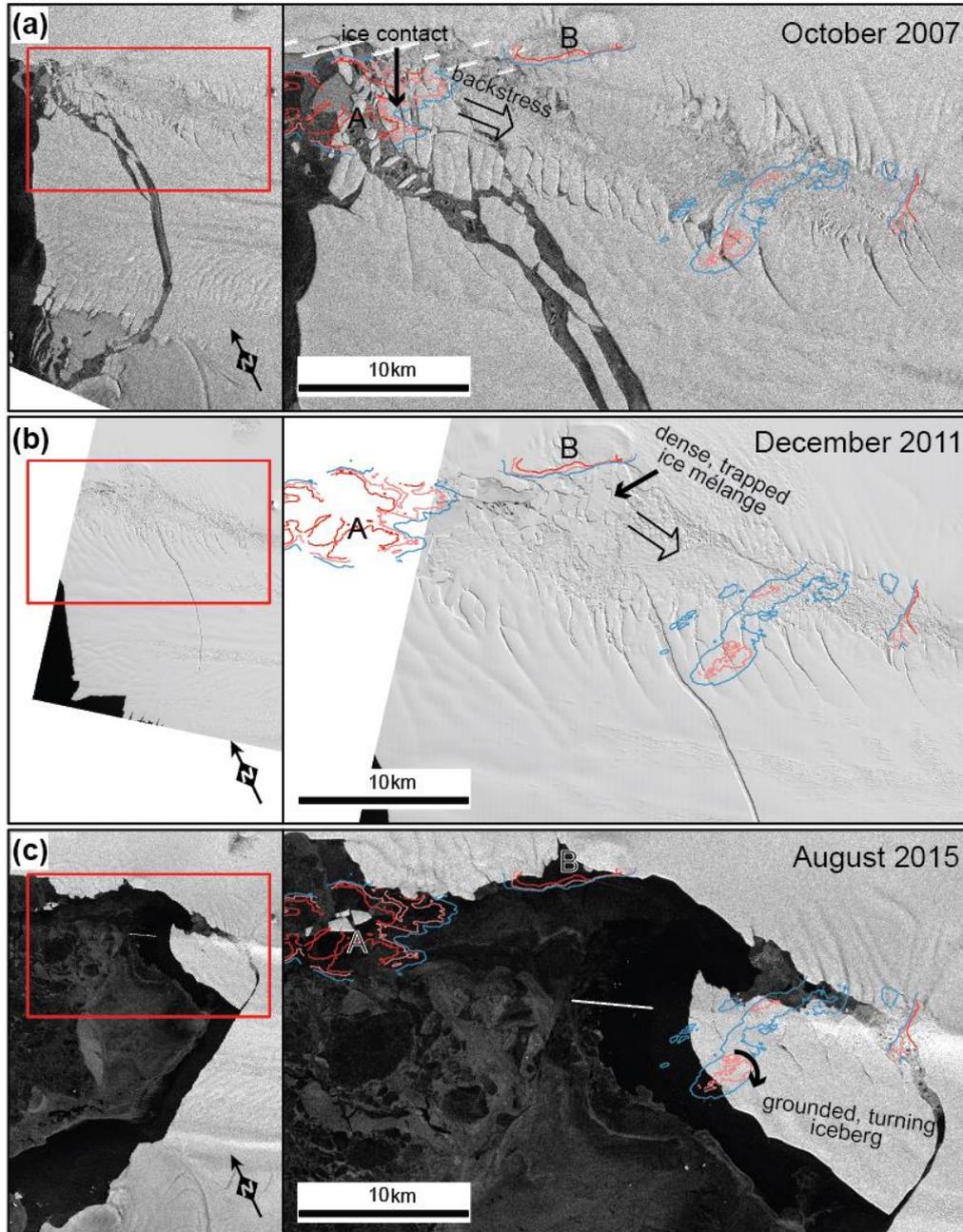
**Figure 4: Time series of satellite images taken shortly before or after iceberg calving events of Pine Island Glacier that took place after 2006 when last imprints of ice contact to the bathymetric ridge were observed. Lines indicate depth contours of 350 m (dark red), 400 m (light red) and 450 m (blue). (a) ERS image taken on 6th of October 2007, note the curved calving line that is induced by back stress affecting the northern part of PIG ice shelf as a result of ice contact with the shallow bathymetry at A. (b) Aster image taken on 22nd of December 2011, note curved calving line probably induced by dense iceberg mélange being trapped between the Northern Ice Shelf near bathymetric high B and Pine Island Glacier. (c) TanDEM-X-SAR image (© DLR2015) taken on 30th of August 2015, note the 1-2 km sized icebergs stuck on shallow bathymetry in top left corner and the stationary large iceberg located on top of the bathymetric ridge.**
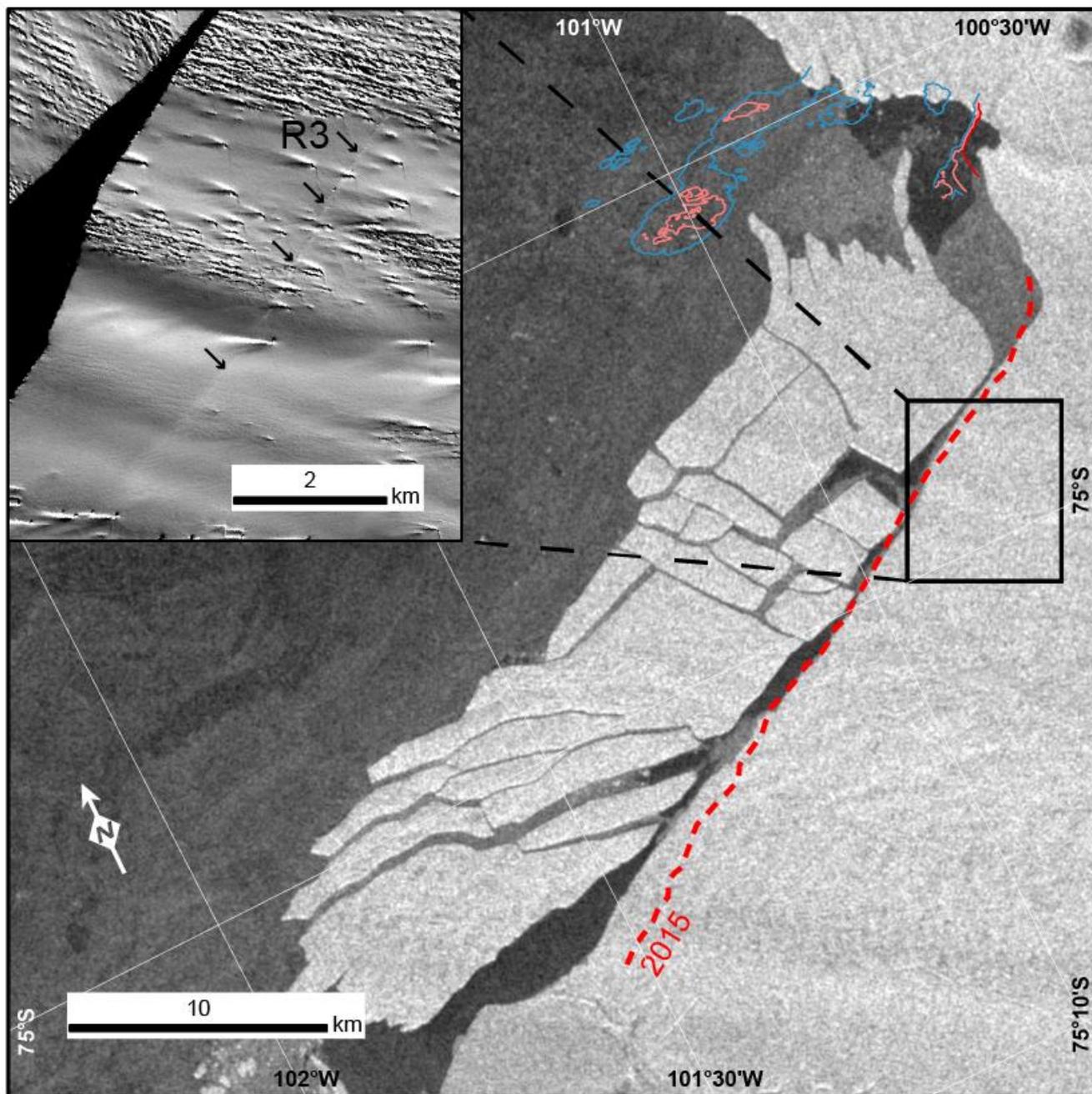
**Figure 5: Sentinel S1 image taken on 11th November 2017 showing the calved and subsequently fast disintegrated iceberg after the 2017 calving event that confirmed the 2015 calving front location and orientation (dashed red line), lines indicate depth contours of 350 m (dark red), 400 m (light red) and 450 m (blue). Inset shows Sentinel S2A image taken at low Sun angle on 13th October 2017 revealing rift R3, for location see black box in main figure.**

**Table 1: SAR and optical satellite imagery used in this study**

**SAR imagery**

| Platform | Sensor | Mode | SAR band | Time interval [yyyy-mm-dd] | Multi-look factors [range x azimuth] | MLI spatial resolution [m] |
|---|---|---|---|---|---|---|
| ERS-2 | AMI SAR | IM | C-band | 2004-10-16 2010-12-04 | 1x5 | ~20 m |
| Envisat | ASAR | IM | C-band | 2006-02-05 2009-10-18 | 1x5 | ~20 m |
| ALOS | PALSAR | FBS | L-band | 2006-11-04 2007-12-29 | 1x3 | ~10 m |
| RADARSAT-1 | SAR | Standard | C-band | 2007-03-01 2008-04-29 | 1x4 | ~20 m |
| TerraSAR-X/ TanDEM-X | SAR | SM | X-band | 2011-09-21 2014-08-28 | 5x5 | ~10 m |
| Sentinel-1A/B | SAR | IW | C-band | 2014-10-10 2017-09-24 | 5x1 | ~20 m |

**Optical imagery**

| Platform | Sensor | Time interval [yyyy-mm-dd] | Spatial resolution [m] |
|---|---|---|---|
| Terra | ASTER (VNIR) | 2005-01-03 2013-02-17 | 15 m |